

Reactive Phase Change Materials for Enhanced Thermal Energy Storage

by
Griffin Drake

A THESIS

submitted to
Oregon State University
Honors College

in partial fulfillment of
the requirements for the
degree of

Honors Baccalaureate of Science in Chemical Engineering
(Honors Scholar)

Presented April 19, 2018
Commencement June 2019

AN ABSTRACT OF THE THESIS OF

Griffin Drake for the degree of Honors Baccalaureate of Science in Chemical Engineering presented on April 19, 2018. Title: Reactive Phase Change Materials for Enhanced Thermal Energy Storage.

Abstract approved: _____

Nick AuYeung

Effective storage and release of low-to-moderate temperature thermal energy (e.g. solar thermal or geothermal) could be transformational for applications such as space heating/cooling, domestic hot water, or off-grid cooking. Good candidates for thermal energy storage in this temperature range include latent heat storage (LHS) systems and thermochemical energy storage (TCES) systems using reversible salt-hydrate dehydration reactions. Here we propose that an energy storage system by use of magnesium nitrate hexahydrate can potentially improve upon independent TCES or LHS systems by utilizing both the thermochemical hydration reaction and the latent heat available through the solid-liquid phase change of one magnesium nitrate hydrate eutectic. This chemistry is investigated through TGA/DSC analysis and shows a total energy density of approximately 1170 ± 94 kJ/kg when dehydrating the material up to 145°C . Reversible latent heat cycling at a eutectic melting temperature of 130°C is shown by the DSC signal and estimated to be on the order of 115 ± 9.2 kJ/kg—a 10% increase over the thermochemical energy storage alone. Although the latent energy release was found to decrease slightly over several cycles, the mass was found to stabilize near an asymptotic value corresponding to the published eutectic composition. These results suggest the concept of reactive phase change materials could be a promising solution to increasing volumetric stored energy density.

Key Words: energy storage, solar thermochemical, phase change materials

Corresponding e-mail address: drakeg@oregonstate.edu

©Copyright by Griffin Drake
April 19, 2018
All Rights Reserved

Reactive Phase Change Materials for Enhanced Thermal Energy Storage

by
Griffin Drake

A THESIS

submitted to
Oregon State University
Honors College

in partial fulfillment of
the requirements for the
degree of

Honors Baccalaureate of Science in Chemical Engineering
(Honors Scholar)

Presented April 19, 2018
Commencement June 2019

Honors Baccalaureate of Science in Chemical Engineering project of Griffin Drake
presented on April 19, 2016

APPROVED:

Nick AuYeung, Mentor, representing Department of Chemical, Biological, and
Environmental Engineering

Greg Herman, Committee Member, representing Department of Chemical,
Biological, and Environmental Engineering

Willie "Skip" Rochefort, Committee Member, representing Department of Chemical,
Biological, and Environmental Engineering

Lucas Freiberg, Committee Member, representing Department of Chemical,
Biological, and Environmental Engineering

Toni Doolen, Dean, Oregon State University Honors College

I understand that my project will become part of the permanent collection of Oregon
State University, Honors College. My signature below authorizes release of my
project to any reader upon request.

Griffin Drake, Author

Reactive phase change materials for enhanced thermal energy storage

(reproduced in part from Energy Technology, “Reactive Phase-Change Materials for Enhanced Thermal Energy Storage,” 2018, vol. 6(2), 351-356. <https://doi.org/10.1002/ente.201700495>).

Introduction

Because peak diurnal and seasonal solar fluxes are misaligned with the demand for low-to-moderate temperature thermal energy for applications like cooking and space heating, solutions for both short and long-term energy storage are needed.

For storage over long timescales, thermochemical energy storage (TCES) using reversible reactions has been proposed. During the charging step, the reaction is run forward, and heat is stored in the chemical potential of the products. The resulting products are separated and stored until there is a demand for thermal energy, at which point the reaction is run in reverse to produce usable heat. There are a wide variety of potential chemistries suited to different temperature applications [1].



Dehydration of salt hydrates is one chemistry that has strong potential for TCES applications. The reactions follow the general form:



Salt-hydrates have several benefits including low toxicity and flammability, relatively high thermal conductivity and wide availability [2]. Many salts have multiple stable hydrate states and lose their waters of hydration in several discrete steps, each step with its own equilibrium temperature [3]. This allows for flexibility in designing for a specific application. For instance, calcium chloride can be dehydrated from the hexahydrate to the tetrahydrate state at a low temperature (30°C); however, it can store additional energy with a transition to the dihydrate (45°C), monohydrate (175°C) or anhydrous phase (260°C). Mixtures of multiple salt-hydrates demonstrated to have improved cycling stability and higher energy densities provide additional customization [4].

For storage on shorter time scales, latent heat storage (LHS) has been extensively studied and implemented in applications such as solar cookers and building materials [5]. Phase transitions happen at a constant temperature, making phase change materials (PCM) ideal for use in systems with stringent temperature specifications. Solid to liquid transitions are generally favored, exchanging much more latent heat than solid-solid transitions while avoiding gas storage problems associated with liquid-gas transitions [2]. PCMs are selected to have a high heat of fusion, specific heat, heat capacity and density, as well as to have a low propensity for supercooling, as some materials will freeze at a lower temperature than their melting points, due to problems with their nucleation and rate of crystallization [2, 6]. Again, stability is an important consideration as extended thermal cycling will often degrade materials [5].

Despite problems of volumetric change and supercooling, salt hydrates remain a viable candidate for LHS for the same reasons why they are attractive for TCES. As opposed to an open system where salt hydrates are dehydrated, LHS utilizes a closed system where salt hydrates are melted. Kong et. al. [2] define the congruent melting of a salt hydrate as an anhydrous salt that is completely soluble in the water of hydration at the melting temperature. In other words, the stoichiometric amount of water removed from the solid crystalline lattice through heating is available to dissolve the newly formed lower hydrate or anhydrous salt. As a result, the melting points of lower hydrated states are greater than that of the fully hydrated state because less water is available as a solvent. Here we propose the removal of water during dehydration to reach a lower hydrated state with a higher melting point. To accomplish this mass loss, considerations of encapsulation will differ from those of conventional LHS systems [7], discussed below.

Magnesium nitrate hexahydrate has been explored for LHS and TCES applications, however, it is usually not considered a strong candidate as it displays a tendency for significant supercooling [8] and is known to decompose to magnesium oxide under strong heating [9]. However, research examining the slow dehydration of magnesium nitrate hexahydrate has shown stable lower hydrate states before eventually decomposing at 400°C [9]. A eutectic composition of 82% magnesium

nitrate/18% water has been found to melt congruently at 130°C [10]. In the solid state, it was calculated that this composition corresponds to 90% dihydrate and 10% anhydrous salt. Interestingly, 130°C is easily achievable with available sources of low grade thermal energy, and it is a useful temperature for residential and humanitarian applications.

It is hypothesized that if this eutectic composition is sufficiently stable, this material could be first dehydrated and then melted, storing both thermochemical and latent heat. A single charging step, then provides two independent options for the release of heat: stored latent heat can be used on a diurnal timescale, while stored chemical energy can be released on demand with the addition of water, compensating for times of low solar availability. Figure 1 illustrates the integrated processes in a block diagram.

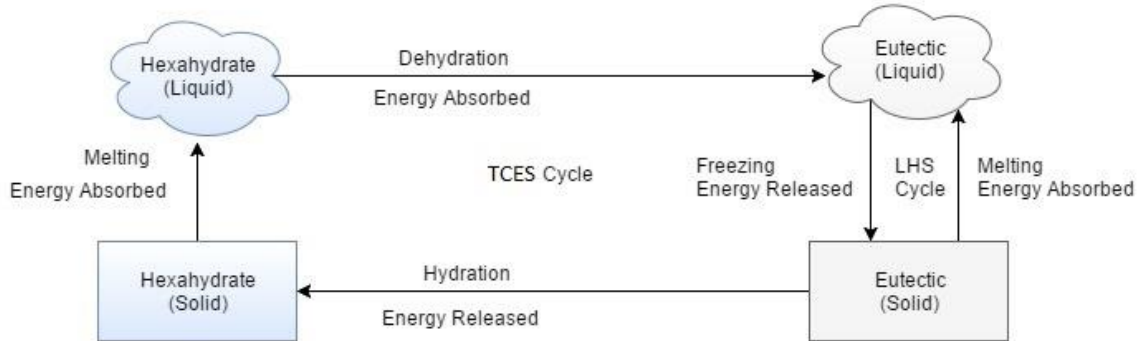


Figure 1: Proposed system for using both thermochemical and latent heat of magnesium nitrate. The TCES cycle includes the freezing step of the LHS cycle, however the LHS cycle can be run independently.

Combining these two energy storage methods harnesses the advantages of both. The theoretical enthalpy of dehydration from the hexahydrate state to the eutectic state is 1410 kJ/kg [11]. To gauge the additional energy that could be harnessed from the latent heat of the melted eutectic, this study aims to measure its heat of fusion. For comparison, however, the heat of fusion of the hexahydrate is published to be approximately 150 kJ/kg [8]. This corresponds to an 11% increase in energy density. As such, there is a strong theoretical and practical base for the exploration of this salt as a TCES/LHS reactive phase change material.

Methods

The energy density and decomposition temperatures of magnesium nitrate hexahydrate was analyzed through TGA/DSC testing. A Netsch STA 449F5 was used with alumina crucibles. Tests were typically conducted using 10-40 mg of hexahydrate salt samples and a 1°C/min or 0.5°C/min heating rate under a flow rate of 40 ml/min argon. A 5-metal temperature and sensitivity calibration was used. All experimental programs were run with blank crucibles to form a correction file; final results have this correction subtracted from the data. Peak onsets and areas were calculated using PROTEUS analysis software. Instrument specifications are given in Table 1.

Table 1: Sensor specifications and instrument uncertainty. TGA uncertainty was estimated by the repeated measurement of a known-weight standard under realistic conditions. DSC uncertainty was estimated from the deviation of known metal standards from the calculated sensitivity curve. Uncertainties in onset temperature measurements, when compared to known metal standards, have been found to be almost negligible. Specifications and further information can be found in [13].

Measurement	Specification	Uncertainty
TGA	0.1 µg resolution	0.338 mg
DSC	± 2% kJ/kg, typical materials	±8% kJ/kg
Temperature	0.001 °C resolution	<0.1 °C

Initial trials were conducted to replicate the dehydration curve of [9] and to associate DSC peaks with the dehydration steps and phase changes, the goal being to provide an estimate of the thermochemical energy capacity and a preliminary analysis of feasible temperature ranges. This was

determined by heating the hexahydrate to 500°C at a rate of 1°C/min. The next phase of trials thermally cycled a sample of hexahydrate salt around the eutectic temperature given in [10]. The salt hydrate was initially heated at 0.5 °C/min to 145°C, which melted and partially dehydrated it to the eutectic composition. Next, it was cooled to 85°C, and reheated for 2 additional cycles. The processes of cooling and heating were intended to induce phase changes, allowing us to examine the LHS system (here referring to the freezing/melting transition of the salt-hydrate) in terms of eutectic composition, potential energy storage, and stability of cycling. Additional cycling tests at alternative temperatures and cycle counts were performed to examine the effect of these variables on LHS storage and salt-hydrate decomposition.

Results

The decomposition of magnesium nitrate hexahydrate was consistent with literature. In the TGA curve of Figure 2, plateaus are seen at $56\pm1.8\%$ (mass percent of initial hexahydrate) from 300-400°C, and at $17\pm1.8\%$ from 450-500°C. Though not strictly a plateau, there is a notable decrease in decomposition rate in the 150-250°C range. There is a single clear peak corresponding to the initial mass decrease with an area of 763 ± 61 kJ/kg. The final large DSC peak corresponds with the final mass decrease and has an area of 729 ± 58 kJ/kg.

In the LHS cycling test, Figure 3, the freezing and melting phase change is clearly visible. The salt-hydrate is first dehydrated to $72\pm2.2\%$ of the initial hexahydrate mass, producing two peaks with areas of 543 ± 43 kJ/kg and 244 ± 20 kJ/kg respectively. As the material cools, a sharp exothermic DSC peak is seen around roughly 115°C, signaling that the salt-hydrate has undergone the freezing transition. As the material is heated, at the beginning of the next cycle, the complimentary sharp, endothermic peak, with an onset of 130°C, signals the salt-hydrate is melting. The presence of alternating peaks shows that the LHS system is reversible. The initial dehydration causes the mass to decrease to $72\pm2.2\%$ of the initial hexahydrate weight, although it continues to decrease to $70\pm2.2\%$ and $68\pm2.2\%$ over the next two heating steps.

Indicating the supercooling effect, there is an obvious disparity in onset temperature of about 15°C between the freezing and melting peaks, and melting temperatures are much more consistent than freezing temperatures. This disparity applies to latent energy as well. Comparing the freezing/melting peak of the first cycle in Figure 3, melting accounts for 85.7 ± 6.9 kJ/kg, while freezing is only 78.3 ± 6.3 kJ/kg.

For high temperature testing, Figure 4, the general pattern of the DSC signal is the same, with distinct freezing and melting peaks, although the initial dehydration has become a single peak of 1120 ± 90 kJ/kg. However, the disparities noted above seem to increase. The material still melts at 130°C in high temperature testing, but does not freeze until 93°C. The LHS cycle peaks for Figure 4 **Error! Reference source not found.** have an 87.6 ± 7.0 kJ/kg endotherm and a 64.2 ± 5.1 kJ/kg exotherm. Agreeing with the results from the lower temperature trial, the final mass after the higher temperature trial was found to be $68\pm1.4\%$.

The extended cycling experiment (Figure 5) again demonstrates the same pattern, but here subtle trends are more visible. There is a slight decay in the magnitude of the LHS peaks, with a 6.3% decrease in melting peaks and a 17% decrease in freezing peaks over the 6 cycles. There is an immediate decrease in freezing onset temperature after the first cycle to 111°C, which continues to decrease until 106°C in the sixth cycle. Melting temperature remains constant at 129°C. The mass decreases over the first two cycles to $68\pm2.0\%$, after which it remains relatively stable with minimal (less than 0.3%) additional losses per cycle.

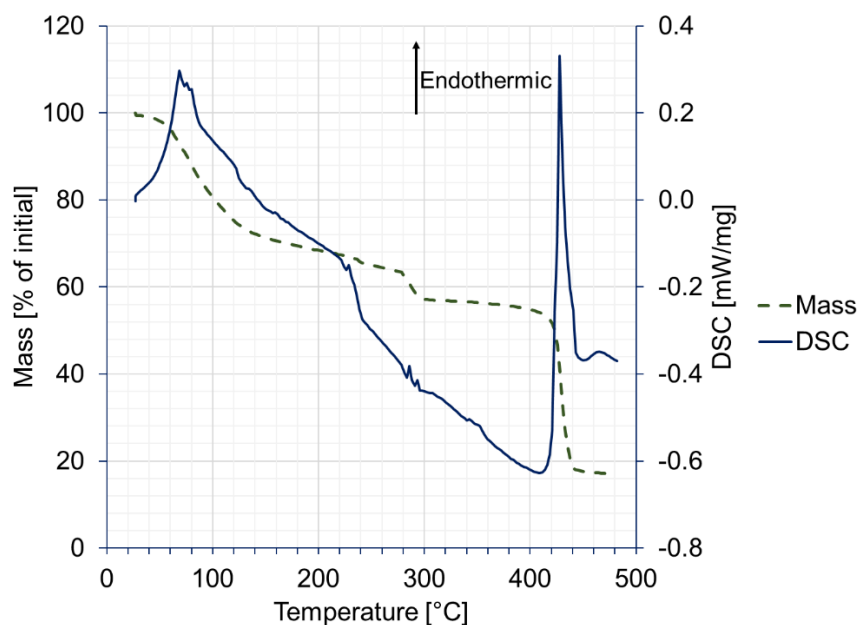


Figure 2: Decomposition of magnesium nitrate hexahydrate at constant 1°C/min.

Table 2: Selected DSC Peaks from Figure 2.

	Initial dehydration	Decomposition
Energy density (kJ/kg initial)	763±61	729±58
Onset temp. (°C)	20.	426

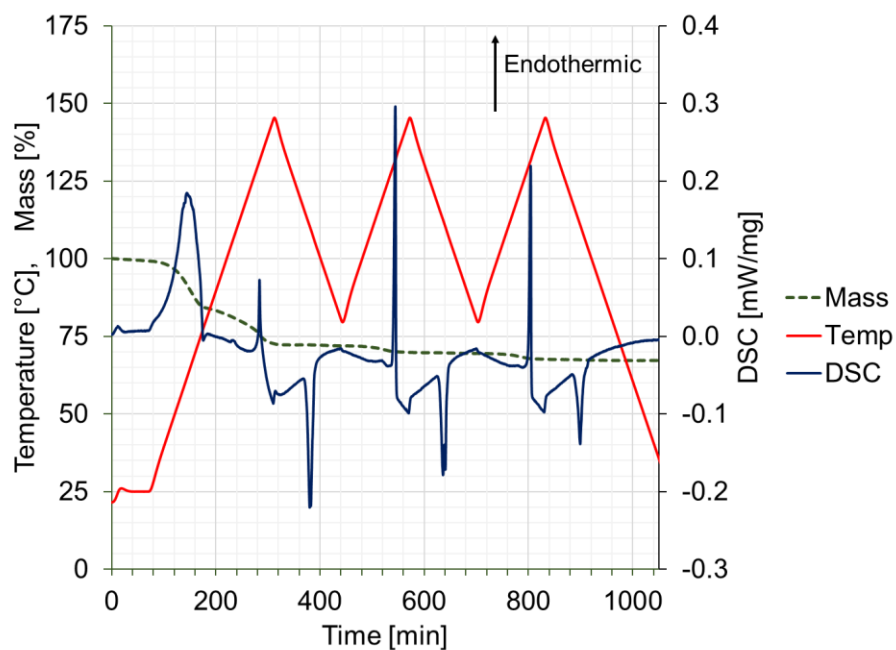


Figure 3: LHS cycling at 145°C of magnesium nitrate hexahydrate. The temperature program decomposes the salt-hydrate to the eutectic composition in the initial step. Following that, the heating and cooling above the melting and freezing points produces sharp DSC peaks that inform the nature of the phase change.

Table 3: Selected DSC peaks from cycling trial (maximum temperature of 145°C) in Figure 3.

Energy density basis	Dehydration 1	Dehydration 2	Freezing 1	Melting 2	Freezing 2	Melting 3	Freezing 3
kJ/(kg initial)	543±44	244±20	101±8.1	85.7±6.9	78.3±6.3	66.8±5.3	59.3±4.7
kJ/(kg final)	808±65	362±29	150±12	128±10	117±9.3	99.4±8.0	88.2±7.1
Onset temp. (°C)	93	130	114	130	116	130	115

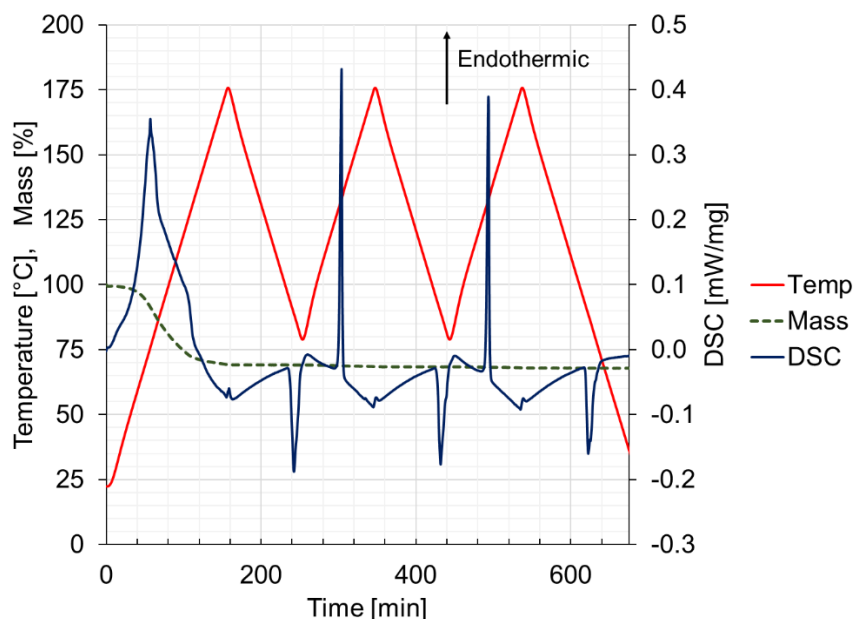


Figure 4: High temperature (175°C) LHS cycling of magnesium nitrate hexahydrate. This test shows a conglomeration of the first two DSC peaks and significantly less melting peak area.

Table 4: Selected DSC peaks from high temperature cycling trial (maximum temperature of 175°C) as shown in Figure 4.

Energy density basis	Dehydration	Freezing 1	Melting 2	Freezing 2	Melting 3	Freezing 3
kJ/(kg initial)	1120±90.	71.2±5.7	87.6±7.0	64.2±5.1	83.4±6.7	67.7±5.4
kJ/(kg final)	1650±130	105±8.4	129±10.	94.6±7.6	123±9.9	99.8±8.0
Onset Temp. (°C)	25	94	130	112	129	92

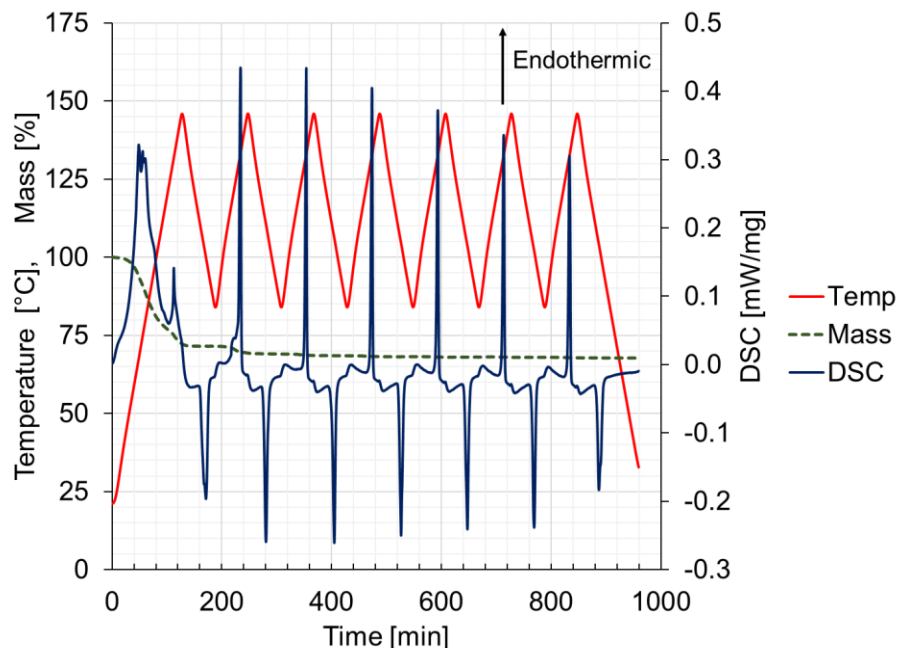


Figure 5: Extended 145°C LHS cycling of magnesium nitrate hexahydrate. A similar pattern to the reduced cycling is seen, although mass appears to stabilize and LHS energy storage appears to decrease.

Table 5: Selected DSC peaks from Figure 5

Energy Density Basis	Melting 1	Freezing 1	Melting 6	Freezing 6
kJ/(kg initial)	123±9.8	82.5±6.6	77.3±6.2	68.6±5.5
kJ/(kg final)	182±14.5	122±9.7	114±9.1	101±8.1
Onset Temp. (°C)	129	115	129	106

Discussion

The results of the TGA/DSC analysis on magnesium nitrate allows us to evaluate its potential as both a TCES and LHS material. The formation of magnesium oxide and the overall reversibility of the material is best seen in the decomposition curve, Figure 2. The literature value for the eutectic (82% anhydrous salt and 18% water) corresponds to 70% of the initial hexahydrate weight. This value, as seen in Figure 2, occurs shortly after the large initial DSC peak. The anhydrous state (57.9%) likely corresponds to the first plateau at 56%. Formation of the oxide (15.7%) corresponds to the final plateau at 17% of the initial weight. From this we can see that the irreversible decomposition does not occur until over 400°C, a limit that can easily be respected in targeted low temperature thermal applications.

The DSC signal for the transition from the dihydrate to the complete anhydride at 270°C in Figure 2 does not display the sizeable endotherm that is expected. This is a contradictory result as the theoretical value for the transition from dihydrate to anhydrous has been calculated to be approximately 190 kJ/kg [11], and previous DTA studies have found endothermic peaks in this region [9]. The peaks here may be obscured by instrument drift. This explanation is plausible, considering Paulik, et. al [9] required the use of quasi-isothermal and quasi-isobaric conditions for adequate resolution. Further characterization of this transition may prove useful; however, this phenomenon does not interest this study because the anhydrous salt will not exhibit moderate temperature LHS capacity.

From the DSC peak areas in Figure 3, the TCES system can be seen to store upwards of 1060 ± 170 kJ/kg of chemical reaction energy at the dehydrated eutectic composition. Energy densities are given based on the dehydrated mass, as the dehydrated mass will be the stored product for application purposes. Reaction cycling on the benchtop scale demonstrates that hydration and dehydration for energy release can be functionally accomplished. Typically, upon the addition of water to a dehydrated salt-based material, the temperature rises rapidly.

The TCES is augmented with approximately 115 ± 9.2 kJ/kg of usable heat of fusion, increasing the total energy stored by roughly 10%. Concerning stability, the LHS shows a decline in energy storage of 17% over six cycles. The loss of energy in the LHS system is likely due to incongruent phase changes, a common effect in salt-hydrate PCMs [2, 8]. When the magnesium nitrate melts, the water is evenly dispersed, but on freezing, the original crystalline structure may not be perfectly reformed, and these different states may have an energy disparity. Since the freezing and melting here is done on a relatively short timescale, it is feasible that the complete phase change may not happen over one cycle, producing the continual decreasing effect seen here. Since this degradation can likely be attributed to a non-homogeneous distribution of water, it is possible that rehydration in slight excess – done to release the TCES energy – could redistribute water through the sample and restore the full LHS capacity.

The loss of energy density is quantified in Figure 6. It is shown that the majority of the energy degradation (14% of the 17% total energy loss) occurs during the first cycle, after which the loss stabilizes at a relatively constant, low value. This persistent, low degree of energy loss suggests that some cycle degradation is inevitable, but is significantly more stable than the initial system losses indicate. If incongruent melting is causing this effect, there

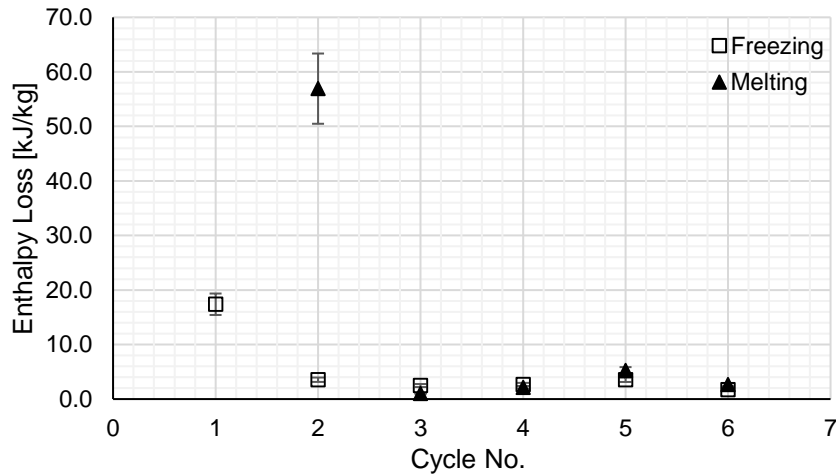


Figure 6: Absolute energy density losses from Figure 5. Energetic losses are high between initial thermal cycles, but stabilize at a low value.

The temperature disparity between melting and freezing peaks is likely due to supercooling effects, as noted earlier. This is an important consideration for practical use of the salt, as the temperature of discharge is critical for applications such as cooking. This may be alleviated using a matrix material, a standard practice in many TCES designs [13]. Porous matrices are typically used to enhance mass transport during sorption and desorption, improve overall conductivity, and encapsulate salt materials for ease of use and avoidances of agglomeration, but they could also likely provide nucleation sites to encourage crystallization. Release temperature was found to degrade as a function of cycling as well, as seen in Figure 7. This suggests that the presence of excess anhydrous salt, a product of incongruent melting, can contribute to a lower release temperature. In practice, since the energy density losses become quite small after a few cycles, this temperature decrease may be the limiting factor for practical use.

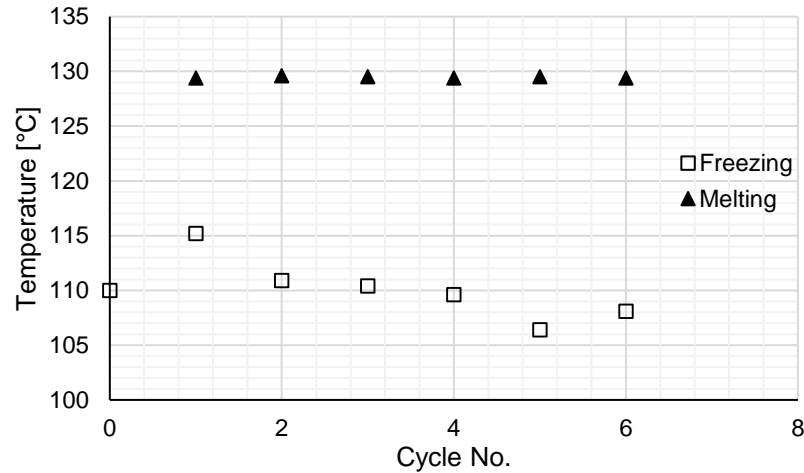


Figure 7: Phase change onset temperatures for associated peaks from Figure 5. Melting temperature stays steady while freezing temperature displays a downward trend. Freezing temperature is the greater concern for practical application.

TCES-inspired matrices appear to be a more appropriate design than LHS-inspired encapsulation, as the latter is designed to limit mass losses from the system [7], a critical component of the desorption step. However, matrices for reactive phase change materials will require specific design modifications to allow for the effective containment of liquid phases and material integrity on expansion. Expanded graphite composites and pyrolyzed melamine-formaldehyde bisulfate copolymer foams (shown in Figure 8) have shown some promise as potential host matrices; improved design and characterization of these matrices is a topic for future work.

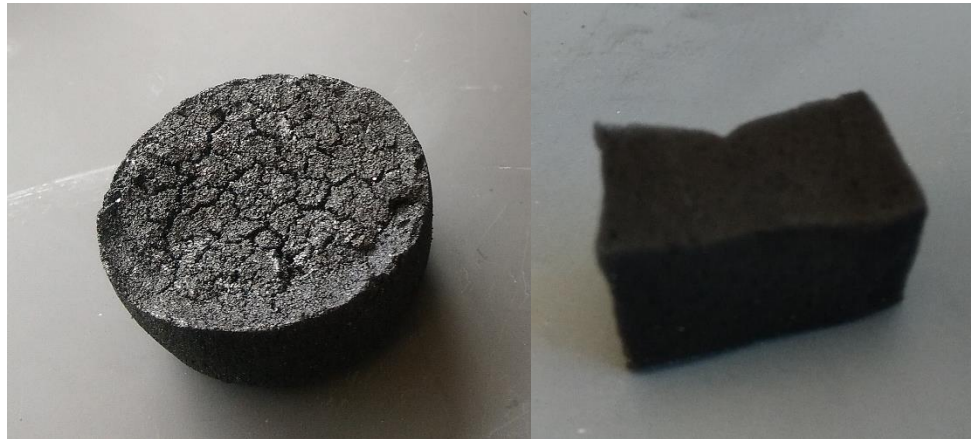


Figure 8: Prototype materials for hosting salt-hydrate materials. Left – expanded graphite composite. Right – flexible, pyrolyzed melamine-formaldehyde foam. Carbon-based materials have the advantage of thermal stability, high porosity, and low cost.

Testing at alternative temperatures shows that the salt-hydrate remains viable and near the required eutectic composition even under non-ideal conditions, allowing for temperature variability in solar desorption. However, since higher dehydration temperatures are associated with increased supercooling and incongruent melting, close regulation of the reaction temperature may be important for functional use. Future work should characterize the severity of this effect to determine the optimum control range.

The mass of the material shows degradation as well, although in comparison to the latent-heat storage capacity, it is relatively stable. This is qualified by the fact that the TGA chamber is subject to a continuous, inert purge gas which may remove small concentrations of water from samples. Incongruent melting may also contribute to this effect, as water which is less evenly distributed through the crystal structure potentially creates weaker intermolecular forces, leaving the

water more vulnerable to vaporization under these hot (greater than 100 °C) conditions. Still, even though no definitive plateau was observed in the decomposition curve (Figure 2) at the expected eutectic composition, the extended cycling experiment demonstrates that the mass nearly stabilizes. This is best expressed in Figure 9. Much like the trend observed in Figure 6, stability is reached after a few cycles, suggesting reasonable potential for long-term use.

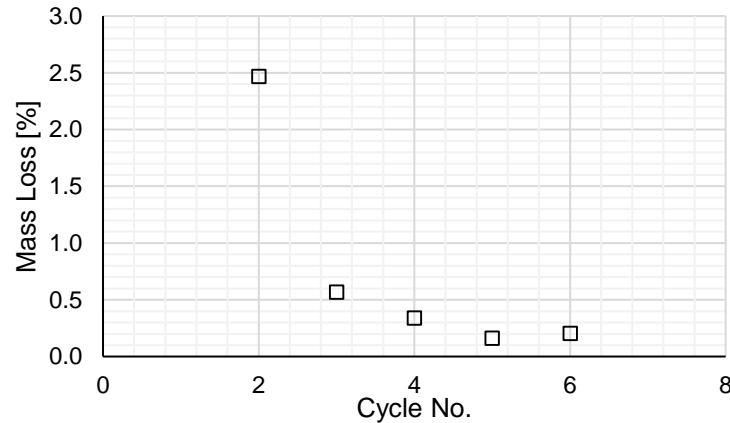


Figure 9: Mass losses from Figure 5. The initial mass loss is omitted for clarity of degradation trends. Mass loss quickly decreases and stabilizes below 0.5% after initial large losses.

Currently, this reactive phase change material is slightly more expensive than other commonly used LHS or TCES materials, however, the final cost will likely be dictated by the host matrix material. Use of reactive phase change materials also means LHS and TCES can be carried out in a single compact reactor, using less salt-hydrate as well as other system materials. This advantage may make a reactive PCM well suited to emerging market applications where material shipping and startup costs can be prohibitive. In addition, the comparatively higher release temperature of this LHS material means the stored energy can be used for more applications, a tangible value addition.

With the material thermally characterized, the next step is to consider its integration into an engineered system for the effective storage, release and utilization of heat. Prototypes of packed-bed sorption reactors have been created for use with calcium chloride or magnesium sulfate [1, 14]. The most common design uses a tubular packed bed of salt-hydrates or salt impregnated matrices. For discharge, use of steam or wet air for rehydration is standard; little work has been done on liquid water systems. Heat is generally captured from the exterior of the reactor or captured by the reactive water stream directly. A flexible reactor with a calcium chloride based chemistry, suitable for both sorption and desorption steps, has proven successful for space heating [15]. Temperatures needed to dehydrate magnesium nitrate (145°C) can be easily reached with existing solar technologies [16]. However, mass transport is an important consideration; if water cannot be effectively removed and separated from dehydrated salt, little energy can be stored. Forced convection will likely be necessary to improve material gradients, while storage will require an air tight environment to prevent deliquescence.

This type of energy storage provided by this specific material is best suited for space and water heating, which require heat at roughly 25°C and 50°C, respectively. There is some potential for cooking applications, but this is strongly limited by the freezing temperature; after accounting for system losses and degradation, the 115 °C release temperature does not provide a large enough margin to meet demands for boiling water. For these low-temperature targets, a shell-and-tube based design should be sufficient. As mentioned Solar-based reactors are considered here, but other heat sources

For space heating, the final design might resemble a traditional flat plate solar collector. Air could be pumped continuously through a pipe lined with an annular bed of salt-in-matrix materials. This flow provides effective mass and heat transfer to the reactive material and this working fluid can be drawn or deposited directly from the home. Space heating applications require a slow release of heat, which can be accomplished by limiting the flow of water to the bed. Passing the inlet stream through a bubbler should provide sufficient moisture for warming an airstream. Desorption can be accomplished by direct heating of the pipes using a shallow parabolic trough, or by passing a solar-heated airstream through the pipes. The latter may be preferable, as it lends itself better to scaling width-wise; packed salt reactors may have challenges with length scaling due to deliquescence.

For water heating, a similar approach applies, although direct contact between the water and the bed may leach salt from the matrices. A more appropriate design would be an annular salt bed separated by a thin wall from a water tank, a design which lends itself to retrofitting existing water heating systems. Water heating requires a higher power output, and the reaction control should reflect this. Mechanically generated vapor, such as through high pressurized nozzles, could be introduced to the base of the heating jacket and drawn through the reactive material with fans. This design is well suited to desorption by introduction of pre-heated air.

Similar systems using sensible or latent heat storage are already in use, and on short timescales, both reactors may need no vapor addition, allowing them to function on latent heat alone, reducing operating costs and challenges when compared to purely thermochemical systems. Unlike purely latent heat systems, however, energy output can be increased on demand to meet need. Both reactors may benefit from a modular design, perhaps by subdividing or containing the packed bed in wire mesh, allowing for easy removal and replacement. This would allow for a storage capacity much greater than the reactor size, and allow for longer sustained thermochemical release (once one modular piece is completely discharged, it could be replaced without disturbing the discharge reaction occurring in the rest of the bed). Modular design also allows for more effective scaling.

Future work likely hinges upon the effective design of a matrix material. As discussed earlier, supercooling and incongruent melting (which may result from improper nucleation) are the two major issues with the salt-hydrate, and matrix-based solutions may be possible. The conductivity, porosity, and volumetric density of this material will likely have a large influence on reactor design, as this will determine the size of modular components, maximum feasible bed thicknesses, and materials of construction.

Material design should be performed in conjunction with small-scale test reactors, similar to those described for space heating applications. The energy densities characterized here are admittedly under very different conditions than those experienced in a bulk bed; determining the real effectiveness of this material (maximum achievable temperature increases, power density, cycle stability) is critical for bringing reactive phase change materials to the next stage of development.

Conclusion

This work shows proof of concept that reactive phase change materials can enhance energy storage. The increased energy densities demonstrated here mean that systems using reactive PCMs may outperform a TCES or LHS system on its own. It also allows for a more versatile application over different time scales. The system has a combined energy density of 1170 kJ/kg, with 1060 kJ/kg of TCES and 115 kJ/kg of LHS. Future work will investigate key steps towards effective applications, such as material cycling integrity, encapsulation in host matrices, integration into prototype reactors and the reduction of undesired effects like incongruent melting and supercooling. It is appropriate to note that unexplored salt hydrates may also exhibit reactive phase change properties and stable eutectic compositions, some of which may be more economically feasible or energetically favorable. Given the wide range of applications and high global demand for thermal energy, it is of great interest to continue investigations of reactive PCMs for the selection and optimization of a robust chemistry.

Contributions

The author would like to recognize Dr. Nick AuYeung and Lucas Freiberg for their assistance in analysis of the results and in developing the language and recommendations outlined in the discussion.

Acknowledgements

We would like to thank the Pete and Rosalie Johnson Internship Program for their generous support of our research. We would also like to thank Asbury Carbons for providing material support (expandable flake graphite).

References

- [1] T. Yan, R.Z. Wang, T.X. Li, L.W. Wang, I.T. Fred, *Renewable and Sustainable Energy Reviews*, **2015**, *43*, 13-31.

- [2] L.B. Kong, T. Li, H.H. Hng, T. Zhang. *Waste Energy Harvesting: Mechanical and Thermal Energies*. Springer Berlin Heidelberg, **2014**.
- [3] G. Balasubramanian, M. Ghommam, M.R. Hajj, W. P. Wong, J.A. Tomlin, I. K. Puri, *Int. J. Heat Mass Transfer*. **2010**, 53, 25, 5700-5706.
- [4] H. U. Rammelberg, T. Osterland, B. Priehs, O. Opel, W. K. L. Ruck, *Solar Energy*, **2016**, 136, 571-589.
- [5] a) B. Zalba, J. M. Marín, L. F. Cabeza, H. Mehling, *Appl. Therm. Eng.* 2003, 23, 251-283. b) M. Kenisarian, K. Mahkamov, *Renewable and Sustainable Energy Rev.*, **2016**, 55, 371-398.
- [6] Y. Wang, Y. Zhang, W. Yang, H. Ji, *Energy Technology*, 2015, 3, 1, 84-89.
- [7] H. Zhang, J. Baeyens, G. Cáceres, J. Degreè, Y. Lv, *Prog. Energy Combust. Sci.*, **2016**, 53, 1-40.
- [8] M. Kenisarin, K. Mahkamov, *Sol. Energy Mater. Sol. Cells*, **2016**, 145, 255-286.
- [9] F. Paulik, J. Paulik, M. Arnold, R. Naumann, *Journal of Thermal Analysis*, **1988**; 34, 3, 627-635.
- [10] W. W. Ewing, J. D. Brandner, B. C. Slichter, W. K. Griesinger, *J. Am. Chem. Soc.*, **1933**, 55, 12, 4822-4824.
- [11] D. D. Wagman, W. H. Evans, V. B. Parker, R. H. Schumm, I. Halow, S. M. Bailey, K. L. Churney, R. L. Nuttall, *Journal of Physical Chemistry Reference Data*, **1982**, 18, 4, 1807-1812.
- [12] Netzsch, "Key Technical Data – STA 449 F5 Jupiter," NGB-0216 Datasheet.
- [13] D. Aydin, S. P. Casey, S. Riffat. *Renewable and Sustainable Energy Rev.*, **2015**, 41, 356-367.
- [14] a) V. M. Van Essen, H. A. Zondag, J. C. Gores, L. P. J. Bleijendaal, M. Bakker, R. Schuitema, W. G. J. Van Helden, Z. He, C. C. M. Rindt, *J. Sol. Energy Eng.*, **2009**, 131, 4, 1004-1014. b) "Characterization of Salt Hydrates for Compact Seasonal Thermochemical Storage": V. M. Van Essen, J. C. Gores, L. P. J. Bleijendaal, H. A. Zondag, R. Schuitema, M. Bakker, W. G. J. Van Helden, *ASME 3rd International Conference on Energy Sustainability proceedings*, **2009**, 2, 825-830.
- [15] D. Aydin, S. P. Casey, X. Chen, S. Riffat. *Energy Convers. Manage.*, **2016**, 121, 321-334.
- [16] M. Jradi, S. Riffat, *Int. J. Low-Carbon Technol.*, **2014**, 9, 214-224.